



Review

Heterogeneous photocatalysis for selective oxidation of alcohols and hydrocarbons

Lang Chen^a, Jie Tang^a, Lu-Na Song^a, Peng Chen^a, Jie He^a, Chak-Tong Au^b, Shuang-Feng Yin^{a,*}^a State Key Laboratory of Chemo/Biosensing and Chemometrics, Provincial Hunan Key Laboratory for Cost-effective Utilization of Fossil Fuel Aimed at Reducing Carbon-dioxide Emissions, College of Chemistry and Chemical Engineering, Hunan University, Changsha, 410082, Hunan, China^b College of Chemistry and Chemical Engineering, Hunan Institute of Engineering, Xiangtan, 411104, Hunan, China

ARTICLE INFO

Keywords:
 Photocatalysis
 Selective oxidation
 Alcohols
 Hydrocarbons
 Heterogeneous photocatalyst

ABSTRACT

Oxygen-containing organics have high potentials in the synthesis of functionalized organics, and their direct generation from alcohols and alkanes by photocatalytic processes under mild conditions has aroused tremendous interest. In the past decades, much progress has been made especially in the area of heterogeneous photocatalysis under visible light irradiation. In this article, we focus on the selective oxidation of alcohols and hydrocarbons into useful oxygen-containing organics, highlighting the recent advances. Despite the achievements, scale-up production of target oxygen-containing organics is not realized due to low catalytic efficiency. The efficacy of a photocatalyst is greatly dependent on its nature, and a slight change of physicochemical properties could result in significant deviation of photocatalytic activity. For better catalyst design, the related mechanistic aspects have to be understood thoroughly. Furthermore, factors such as reactor design and reaction conditions (e.g. light region and intensity, solvent, oxidant) are critical for optimization of performance. To realize practical application in organic synthesis, it is essential to clarify the underlying mechanism. Once the parameters for optimal performance have been determined, the design of an efficient photocatalytic reactor could be properly considered.

1. Introduction

With high modifiability, oxygen-containing organics are widely used in chemical and pharmaceutical industries. The generation of them by selective oxidation of the corresponding hydrocarbons has been regarded as viable and element economical. Nonetheless, it is hard to achieve high activity and selectivity simultaneously using traditional thermal-catalytic methods. It is because under reaction conditions that are relatively severe, a high reactivity would mean low product selectivity. On the contrast, the conditions for photocatalytic reactions that use visible light to promote organic transformation are mild (e.g. room temperature and ambient pressure). The approach is not only green but also enables high selectivity to target product.

Since the first report on photocatalytic oxidation of aromatic compounds on TiO₂ under UV light [1], photocatalysis has become popular in organic synthesis. Photocatalysis can be homogeneous as well as heterogeneous. Relatively speaking, despite higher in activity, homogeneous photocatalysts such as ruthenium-tri(bipyridine), iridium-tris(phenylpyridine), eosin, and rhodamine-6 G are more expensive and hard to separate from products [2,3]. Since the pioneer work of Zhao

and co-workers using dye sensitized TiO₂ as efficient photoredox catalyst for alcohol oxidation under visible light [4–6], visible-light-driven heterogeneous photocatalysts (e.g., TiO₂, bismuth-containing semiconductors, g-C₃N₄, and composites based on them) have become popular. Compared to homogeneous photocatalysts, the heterogeneous ones are cheaper to make and can be readily separated for reuse. From the viewpoint of industrial production, the use of heterogeneous photocatalysts is advantageous. In this article, we focus on the use of heterogeneous photocatalysts for selective oxidation of alcohols and hydrocarbons into useful oxygen-containing organics, highlighting the recent advances. The paper is divided into 4 parts on the basis of substrates, viz., alcohols, benzene, cyclohexane, and other hydrocarbons with sp³ C–H bonds. We conduct discussion on achievements as well as drawbacks. At the end, we give a short prospect of photocatalysis in organic synthesis.

* Corresponding author.

E-mail addresses: sf_yin@hnu.edu.cn, yinsf73@163.com (S.-F. Yin).

2. Applications of heterogeneous photocatalysts in selective oxidation of organics

2.1. Selective oxidation of alcohols into aldehydes

In heterogeneous photocatalysis, the partial oxidation of alcohols to aldehydes and/or ketones, especially that of benzyl alcohol to benzaldehyde, has been well studied. Since the first report on the selective oxidation of higher alcohols to aldehydes over TiO_2 under UV irradiation by Fujihira et al. [1], much attention has been paid to TiO_2 -based photocatalysts. Despite TiO_2 is biologically and chemically inert and stable, it loses its photocatalytic activity when there is the accumulation of products on its surface. If a reaction is performed in liquid phase with or without a solvent, the accumulation of surface species is less severe. In recent years, efforts were put in to improve photocatalytic activity and selectivity under milder and greener conditions while making fuller use of solar energy. For example, the first attempt of selective oxidation of 4-methoxybenzyl alcohol to aldehyde in aqueous solution over TiO_2 was by Palmisano and coworkers, and selectivity to aldehyde was limited to ca. 41% under visible light irradiation [7]. It is understandable because with a valence band position of about 2.7 eV, TiO_2 is a powerful oxidation agent and hence the poor selectivity. Nonetheless, Colmenares et al. achieved 90% selectivity to benzaldehyde over Fe_3O_4 -supported TiO_2 ($\text{TiO}_2/\text{maghemite-silica}$) using acetonitrile as solvent [8]. Similar solvent effect was reported by others [9–11]. It was observed that the use of acetonitrile would result in a so-called “shield effect” [11]. In such a case, acetonitrile acts as a weak base to stabilize reaction products via solvation, inhibiting proton transfer and preventing the formation of radical species to avoid undesired side reactions. To improve visible light absorption ability and charge carriers separation efficiency, dyes [4–6,12–14] or semiconductors of narrow band gaps (e.g., CdS , AgBr) [15–17] were used to sensitize TiO_2 . Most recently, Li and coworkers reported the deposition of CdS quantum dots on TiO_2 nanocrystals with exposed (001) facets [8]. Because of the photosensitizing effect of CdS quantum dots, the composite displayed strong visible light absorption ability and exhibited high activity in the oxidation of benzylic alcohols with conversions up to 100% and selectivity higher than 98% using benzotrifluoride as solvent. The authors ascribed the high activity to vacancies on the TiO_2 (001) facets that enhance the adsorption of reactants. What is more, the created heterojunctions improve activity by preventing the recombination of charge carriers. The main active species in this reaction system is $\cdot\text{O}_2^-$ rather than $\cdot\text{OH}$ (which has long been regarded as strong but non-selective oxidant), which could be the main reason for the high selectivity.

Besides the TiO_2 -based photocatalysts, there are other photocatalysts tested for this reaction, such as carbon quantum dots [18], $\text{VO}@\text{g-C}_3\text{N}_4$ [19], $\text{g-C}_3\text{N}_4$ and Fe doped $\text{g-C}_3\text{N}_4$ [19,20], ZnIn_2S_4 [21], $\text{BN/In}_2\text{S}_3$ [22], bismuth-containing semiconductors [23–25], CdS [26], Nb_2O_5 [27], non-stoichiometric $\text{W}_{18}\text{O}_{49}$ [28], metal-organic frameworks [29], $\text{C}_3\text{N}_3\text{S}_3$ [30], In_2S_3 [31] and many others. Their performances are summarized in Table 1. Unlike the TiO_2 -based photocatalysts, most of these photocatalysts have relatively mild oxidation capacity and show much higher selectivity towards the partial oxidation products. For example, with a valance band position of 1.4 V, mesoporous C_3N_4 is not capable of oxidizing $-\text{OH}$ (or H_2O) to hydroxyl radicals ($E^\circ (-\text{OH}/\cdot\text{OH}) = 2.4 \text{ V}$) which is rather nonselective in oxidation.

With no generation of $\cdot\text{OH}$ over $\text{g-C}_3\text{N}_4$ in aqueous solution, selectivity to benzaldehydes is high in the oxidation of benzyl alcohols under visible light irradiation (Fig. 1) [20]. Most recently, Au-modified BiOCl was reported to be highly efficient for the selective oxidation of benzyl alcohol in which both $\cdot\text{O}_2^-$ and plasmonic hot holes are indispensable for achieving high activity and selectivity [25]. It was considered that the oxygen vacancies (denoted as OV in Fig. 2) on BiOCl enhanced O_2 adsorption, and facilitated $\cdot\text{O}_2^-$ formation through the

provision of plasmonic hot electrons. With the increase of Au loading, there is enhanced transfer of oxygen atoms from O_2 to the product. At the same time, hot holes on the Au surface mildly oxidized benzyl alcohol to the corresponding carbon-centered radicals followed by the final formation of benzaldehyde (Fig. 2). The synergy is that the Au particles provided the adsorbed O_2 with hot electrons and prevented O_2 from dissociation on the oxygen vacancies.

Despite the great number of reports on photocatalytic oxidation of alcohols to aldehydes and/or ketones under visible light irradiation, to concomitantly achieve high conversion of alcohols and high selectivity to target products remains a big challenge. There is a need to develop efficient photocatalysts that can maximize the absorption of solar energy while fully utilize the generated charge carriers. Additionally, the oxidation capacity of photocatalysts has to be regulated, and the oxidative species monitored. For example, the presence of nonselective oxidation species such as $\cdot\text{OH}$ has to be eliminated to avoid over oxidation.

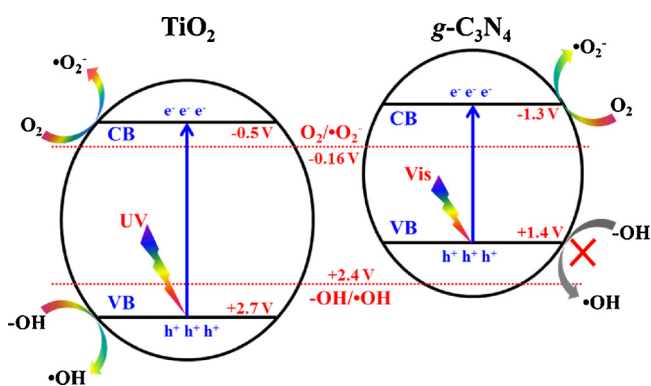
Compared to the selective oxidation of benzyl alcohols, that of aliphatic alcohols or secondary alcohols is more important in organic and pharmaceutical industries, and the conversions are more challenging owing to their poor activity. Distinct from the selective oxidation of aromatic alcohols to aldehydes, that of methanol resulted in the generation of formaldehyde as well as methyl formate. Huang and coworkers studied photocatalytic oxidation of methanol on rutile TiO_2 (110) surface by means of thermal desorption spectroscopy and X-ray photoelectron spectroscopy. They provided direct spectroscopic evidence for the formation of methyl formate as a product of photocatalytic cross-coupling of chemisorbed formaldehyde and methoxy species. During the photocatalytic oxidation of methanol, there is the photocatalytic dissociation of chemisorbed methanol to methoxy species [32]. Liang et al. [33] found that CuO/CuZnAl hydrotalcites-ZnO showed high activity for the production of methyl formate from methanol. A maximum methyl formate yield of 50% at 30 °C with CO_2 being the only by-product was achieved under UV light irradiation. In this process methoxy formation is a key step and a proper redox capacity of the valance band of ZnO is essential. Unlike the short-chain aliphatic alcohols, those with long chains can be converted to the corresponding esters under neutral conditions using visible light as irradiation source. Zhu and co-workers prepared gold-palladium alloy nanoparticles on a phosphate-modified hydrotalcite support which as a photocatalyst can direct oxidative esterification of 1-octanol under base-free conditions [34,35]. Recently, they developed a photocatalyst of mixed-valence vanadium oxide for the production of aldehydes and ketones with high selectivity (35% to 96% for a variety of substrates) from aliphatic alcohols using molecular oxygen as oxidant at mild conditions [36]. Most recently in 2018, up to 90% conversion of three main aliphatic alcohols (1-pentanol, 1-hexanol and 1-heptanol) and nearly 100% selectivity to the corresponding aldehydes was achieved by Xie et al. over a BiOCl photocatalyst at room temperature [37]. Based on results obtained over bismuth oxyhalides, a possible reaction oxidation mechanism was proposed. This work may add enthusiasm in the studies of selective oxidation of aliphatic alcohols in the coming years.

In traditional noncatalytic method for benzyl alcohol oxidation, environmentally unfriendly oxidants such as permanganate and dichromate are used. In photocatalytic processes, it is O_2 that is used as oxidant, giving CO_2 , H_2O and/or H_2O_2 as byproducts. However, there is competition between partial and complete oxidation, resulting in complication and poor efficiency. Even with success in the development of photocatalysts that are high in activity, selectivity and stability, there are technical problems to tackle before industrialization. The scaling up of a photocatalytic process is obviously different from that of a thermocatalytic one, especially in the transfer of light, heat and mass.

Table 1

Summary of lately developed photocatalysts and their performance for the selective oxidation of benzyl alcohol.

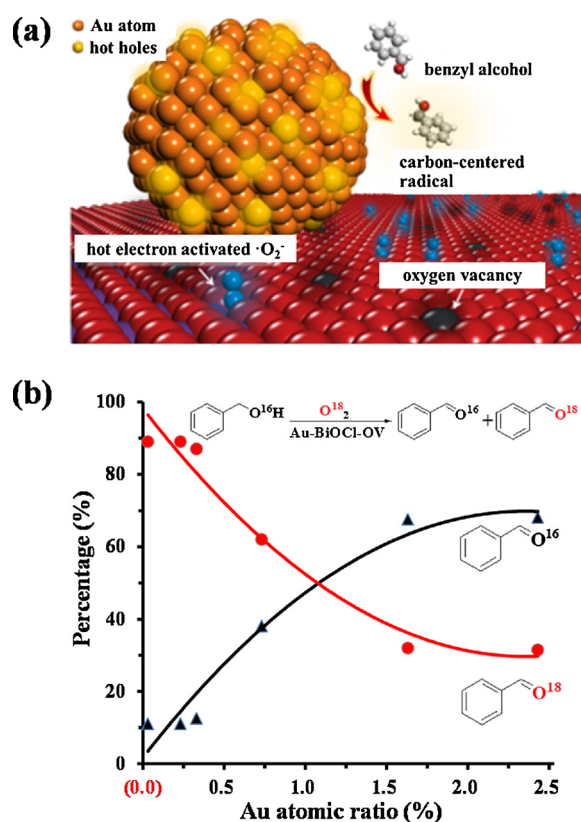
Entry	Photocatalyst	Reaction conditions	Benzyl alcohol/mmol	Sel./%	Yield/%	Ref.
1	25 wt%TiO ₂ /MAGSNC (150 mg)	125 W mercury lamp, acetonitrile solvent, Air (25 mL/min), 30 °C, 4 h	0.225	90	45	[8]
2	CdS/TiO ₂ (50 mg)	300 W Xe Lamp ($\lambda > 420$ nm), BTF solvent (10 mL), O ₂ , 25 °C, 3 h	0.2	100	95	[17]
3	CQDs (8 mg)	450 W Xe Lamp ($\lambda > 700$ nm), H ₂ O ₂ (1 mL), 60 °C, 12 h	10	100	92	[18]
4	VO@g-C ₃ N ₄ (25 mg)	40 W domestic bulb, H ₂ O ₂ (1.5 mmol), acetonitrile solvent (2 mL), 1 h	1	—	98	[19]
5	mpg-C ₃ N ₄ (50 mg)	300 W Xe Lamp ($\lambda > 420$ nm), trifluorotoluene solvent (9 mL), O ₂ (0.8 MPa), 100 °C, 3 h	1	99	57	[20]
6	ZnIn ₂ S ₄ (80 mg)	300 W Xe Lamp ($\lambda > 420$ nm), BTF (2 mL), O ₂ (0.1 MPa), 70 °C, 2 h	0.5	86.1	60.1	[21]
7	7%BN/In ₂ S ₃ (80 mg)	300 W Xe Lamp ($\lambda > 420$ nm), BTF solvent, O ₂ (0.1 MPa), 3 h	0.5	99	59	[22]
8	Au/Ni ₅ AlHT (50 mg)	500 W halogen lamp, 1,4-dioxane solvent (5 mL), O ₂ (1 atm), 40 °C, 24 h	0.5	99	41	[23]
9	BiVO ₄ (32.3 mg)	30 W blue LED, acetonitrile solvent (9 mL), O ₂ (1 atm), 40 °C, 3 h	0.1	100	73	[24]
10	Au-BiOCl-OV (50 mg)	300 W Xe Lamp ($\lambda > 420$ nm), acetonitrile solvent (10 mL), O ₂ (0.1 MPa), 8 h	0.5	99	75.6	[25]

Fig. 1. A comparison of band positions between TiO₂ and g-C₃N₄. [After J. Am. Chem. Soc. 132 (2010) 16299–16301].

2.2. Selective hydroxylation of benzene into phenol

Phenol is in high demand in chemical industries. The current production of phenol is by the multi-step Hock process (also known as cumene-phenol process) using benzene as starting material. This method suffers from drawbacks such as severe reaction conditions, low yield of phenol and a great number of byproducts (acetone and α -methylstyrene). Hence there is an urgent need to develop methods for efficient phenol production. There are methods reported for the catalytic hydroxylation of benzene to phenol [38,39]. However, because thermodynamically phenol is easier to be oxidized than benzene, the development of a one-step process for efficient production of phenol is a formidable challenge [40]. Despite reports on benzene hydroxylation to phenol can be dated back to the early 1960s, there are no processes that are realistic enough for industrial application because of drawbacks such as poor catalytic efficiency and low selectivity to target product [41].

Recently, there are works on the photocatalytic oxidation of benzene to phenol [42–45] (summarized in Table 2). They are the direct hydroxylation of benzene (replacing one H atom of aromatic by OH), and the indirect one involving the hydrolysis of a substituent on the aromatic ring. The latter is similar to a traditional multi-step thermo-catalytic process in which hydroxylation activity is substituent related. Compared to the latter, the former is more atom-economical, but technically more challenging. The commonly used oxidants are molecular oxygen, H₂O₂, N-oxides (e.g., N₂O), and a number of N-containing heteroaromatic bases. As for N-oxides, they also serve as photosensor and there is no need of a photocatalyst for the production of indispensable atomic oxygen. The disadvantage of using N-oxides of heterocyclic bases is that under UV light irradiation they undergo rearrangement rather than release of atomic oxygen. The photolysis of

Fig. 2. (a) The generation of reactive species on Au-BiOCl-OV, and (b) relative proportion of ¹⁸O-labeled benzaldehyde along with the increase of Au loading over Au-BiOCl-OV. [After J. Am. Chem. Soc. 139 (2017) 3513–3521].

heterocyclic N-oxides is greatly dependent on the selection of solvent [46], inevitably limiting their application.

The use of Fenton's reagent (Fe²⁺-H₂O₂) for benzene oxidation to phenol has been known for more than 100 years. This oxidation system strongly depends on the use of acids (such as HClO₄, H₂SO₄, CF₃COOH), and product separation is known to be difficult. In 2009, Wang and coworkers reported the use of Fe-doped g-C₃N₄ (Fe-g-C₃N₄) as photocatalyst for the oxidation of benzene under visible light in the presence of H₂O₂ [40]. On the surface of the photocatalyst, there is the reduction of Fe³⁺ to Fe²⁺ by electrons photogenerated on the CB of g-C₃N₄, and the resulting Fe²⁺ interacts with H₂O₂ to generate ·OH for the production of phenol. Furthermore, it was demonstrated that photocatalytic activity could be enhanced by loading Fe-g-C₃N₄ on porous SBA-15 for increased exposure of active sites. Lately, the researchers

Table 2

Summary of lately developed photocatalysts and their performance on the direct hydroxylation of benzene.

Entry	Photocatalyst	Reaction conditions	benzene/mmol	Sel./%	Yield/%	Ref.
1	TiO ₂ (10 mg)	300 W Hg lamp ($\lambda > 320$ nm), Buffered aqueous solution (10 mL), 40 °C, 6 h	0.02	81	34	[55]
2	TiO ₂ @MCF/CH ₃	300 W Xe Lamp ($\lambda > 320$ nm), Acetonitrile and H ₂ O (29.7 mL), 2 h	0.009	34.7	–	[56]
3	Au/TiO ₂ (60 mg)	1 solar-power light, 2.3 MPa CO ₂ , 34 °C, 24 h	0.13	89	13	[42]
4	Au/TiO ₂ (50 mg)	300 W Xe Lamp ($\lambda > 400$ nm), H ₂ O (100 mL), 0.01 M NaOH and 3.0 mM terephthalic acid.), 3 h	0.8	91	63	[43]
5	Pt(0.1)/TiO ₂ (R) (0.2 g)	300 W Xe Lamp ($\lambda > 385$ nm), H ₂ O (4 mL), 25 °C, 1.5 h	0.57	91	2.1	[44]
6	Au/TiV ₂ (30 mg)	400 W mercury lamp (200–400 nm), CH ₃ CN (2 mL), H ₂ O ₂ (25%, 2 mL),	11	88	15.9	[45]
7	Fe-g-C ₃ N ₄ (50 mg)	500 W Xe Lamp ($\lambda > 420$ nm), acetonitrile solvent (4 mL), H ₂ O (4 mL), H ₂ O ₂ (5 mmol), 60 °C, 4 h	9	100	4.8	[40]
8	Fe-CN/TS-1 (50 mg)	300 W Xe Lamp ($\lambda > 420$ nm), CH ₃ CN (4 mL), H ₂ O (4 mL), H ₂ O ₂ (0.51 mL),	9	18.4 ^a	10	[47]
9	Pt/WO ₃ (10 mg)	300 W Xe Lamp ($\lambda > 420$ nm), H ₂ O (7.5 mL), Air (1 atm), 4 h	0.02	73.7	50.8	[60]
10	MIL-100(Fe) (10 mg)	300 W Xe Lamp ($\lambda > 420$ nm), CH ₃ CN/H ₂ O (1:1, 4 mL), H ₂ O ₂ (39 μL), 8 h	0.5	96	21	[50]
11	Bi ₂ WO ₆ /CdWO ₄ (50 mg)	300 W Xe Lamp ($\lambda > 400$ nm), CH ₃ CN (3 mL), H ₂ O (100 μL), O ₂ (3 mL/min)	0.5	99.9	5.8	[61]

^a Selectivity based on H₂O₂.

prepared Fe-C₃N₄/TS-1 hybrid materials using TS-1 zeolite as support and achieved desirable activity, further confirming that a larger specific surface area could result in higher activity [47]. Earlier on, Zhang et al. dip-loaded FeCl₃ on mesoporous g-C₃N₄, and used the composite to photocatalyze benzene oxidation using H₂O₂ as oxidant under optimized conditions. They reported TOF (based on Fe) much higher than that of Fe-g-C₃N₄/SBA-15. They also investigated the Fe²⁺-induced reduction process of H₂O₂ to ·OH [48]. Nonetheless, the stability of FeCl₃ on the surface of mesoporous g-C₃N₄ is a matter of concern. Because of the lack of strong chemical interaction between FeCl₃ and g-C₃N₄, iron leaching could occur during reaction. To tackle this problem, Xu et al. [49] as well as Wang et al. [50] synthesized Fe-based metal-organic frameworks (the well-known Materials of Institut Lavoisier MIL) as efficient photocatalysts (denoted as Fe-MILs) for benzene conversion using H₂O₂ as oxidant. In terms of H₂O₂ efficiency under visible light irradiation, Fe-MILs (26%–58.5%) are superior to Fe-g-C₃N₄/SBA-15 (20.7%) and Fe-C₃N₄/TS-1 (18%). It is worth pointing out that Fe-MILs are highly reusable and the problem of Fe leaching was solved by having FeO₆ octahedra enclosed inside the metal-organic frameworks.

Compared to the use of H₂O₂, the use of H₂O as hydroxylating agent is much more environment friendly. It was showed that benzene can be photocatalytically converted to phenol in aqueous solution without the use of H₂O₂. Having h⁺ reacting with H₂O, there is the generation of ·OH that directly hydroxylates benzene into phenol. However, the photo-generated ·OH radicals are highly oxidative, and selectivity to the target product is poor, resulting in benzene being converted to unwanted phenolic compounds (such as benzoic acid, hydroquinone and polymerized products from phenolic) and/or CO₂ [51]. Efforts were put in to prevent deep oxidation. Using Au-Pd alloy nanoparticles (Au_{shell}-Pd_{core}) supported on TiO₂ as photocatalyst, Su et al. obtained results superior to those of bare TiO₂; the evolution rate of phenol significantly increased while that of hydroquinone decreased. However, there was still a large amount of undesired by-products and the role of the metal co-catalysts in boosting phenol selectivity was unclear [52]. In the work of Yuzawa and Yoshida with the use of H₂¹⁸O, only 90% of the produced phenol contained ¹⁸O, indicating that either lattice or surface oxygen of TiO₂ was also involved [53]. Furthermore, Bui et al. used ¹³C₆H₆ and ¹³C₆H₅OH to investigate the pathways for benzene oxidative mineralization over anatase and rutile powders [54]. It was considered that the use of water as oxygen source is relevant even though there is distinction in activity owing to difference in energy level and/or atomic configuration on anatase and rutile. With surface

structure more irregular than that of rutile, anatase particles favor the formation of Ti-O·, Ti–OO· and surface peroxides, leading to the formation of phenol. When O₂ was used as oxidant, the discrepancy between the use of anatase and rutile particles is not as significant. Despite both water and oxygen were used in this work, their oxidation capacity was not determined.

In a photocatalytic process, the nature of interactions between reactant, intermediate, product and photocatalyst are critical in terms of activity as well as product selectivity. Shiraishi and coworkers found that the adsorption of benzene on TiO₂ is strong while that of phenol insignificant. A fast desorption of phenol would means high phenol selectivity because further hydroxylation on catalyst surface was avoided [55]. In the work of Choi and coworkers [56], the surface of TiO₂ was modified by silylation agent to make it hydrophobic. In such a case, both the adsorption of benzene and desorption of phenol are facilitated, and the outcome was acceleration of reaction and high selectivity to phenol. It is a clever strategy for selective transformation of a reactant to product with the latter being less strongly adsorbed.

Over TiO₂-based photocatalysts, benzene oxidation in the presence of O₂ usually results in low phenol selectivity [57–59]. In view that the presence of O₂ is common, it is of great significance to determine how oxygen sources influence the oxidation of benzene in photocatalysis. Tomita et al. reported that Pt/WO₃ was an efficient catalyst for selective oxidation of benzene to phenol [60], displaying phenol selectivity much higher than that of TiO₂ or Pt/TiO₂ under similar reaction conditions (Fig. 3). The authors investigated the difference between Pt/WO₃ and Pt/TiO₂ from the viewpoints of surface structure, band gap property and reaction pathway. In both cases, ·OH generated from the interaction of h⁺ with adsorbed water played a dominant role in the oxidation of benzene. Despite the valance band gaps of WO₃ and TiO₂ are similar the reactions on Pt/TiO₂ and Pt/WO₃ are different. Due to interaction with surface hydroxyl groups, benzene molecules adsorbed strongly on TiO₂, whereas on WO₃, benzene adsorption is weak. A good portion of the holes generated on Pt/TiO₂ directly react with benzene molecules, generating cationic radicals which react with O₂ (or ·O₂[–]) to give peroxy radicals. The peroxy radicals are unstable and spontaneously decompose to intermediates, leading to CO₂ formation. The photo-excited electrons on the conduction band of TiO₂ reduce O₂ to radical species such as ·O₂[–] or ·HO₂, which participate in the decomposition of benzene and intermediates. Based on the reaction results using ¹⁸O-labeled H₂O and O₂, the reaction of surface h⁺ with H₂O molecules on Pt/WO₃ primarily generates ·OH radicals that selectively react with

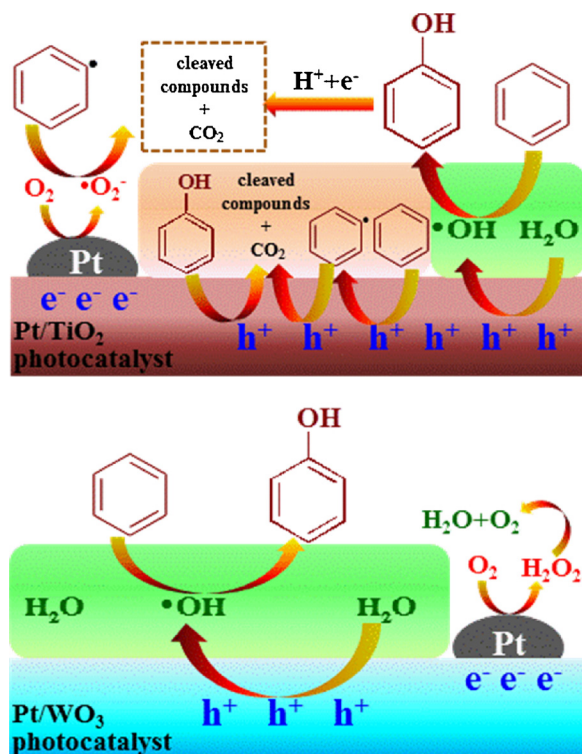


Fig. 3. Possible reaction mechanism for phenol production over Pt/TiO₂ and Pt/WO₃. [After Catal. Sci. Technol. 4 (2014) 3850–3860].

benzene to produce phenol.

Despite all the efforts for selective oxidation of phenol over TiO₂-based photocatalysts, phenol selectivity is still below 80%. Attention has been directed to semiconductor materials that are milder than TiO₂ in oxidation capacity and are endowed predominately with ·OH radicals upon light irradiation. In the engineering of materials with suitable band gap energy and proper oxidation ability, we fabricated 3-dimensional CdWO₄ microrods that are decorated with Bi₂WO₆ nanoplates [61]. The hierarchical composite of the heterostructure enabled phenol selectivity of up to 99% in benzene oxidation with reaction pathway distinct from that of TiO₂. The CdWO₄ support is not excited by light irradiation. On Bi₂WO₆, the photogenerated holes on valence band directly activate benzene to phenyl radicals, while that on conduction band produce ·OH radicals upon interaction with adsorbed water molecules. The phenyl radicals reacted with O₂ or ·O₂[−] and the ·OH with benzene to produce phenol (Fig. 4). However, the disadvantage of this system is that benzene conversion is unsatisfactorily low. To enhance benzene conversion, a way has to be developed to increase the adsorption capacity of reactants as well as the catalytic action of intermediates. Considering the polarity difference between benzene and phenol, it is envisioned that it is possible to modify the surface nature of a photocatalyst to enhance benzene adsorption and to promote phenol desorption. Research work of this kind is being conducted in our group.

2.3. Selective oxidation of cyclohexane to cyclohexanone and cyclohexanol

The partial oxidation of cyclohexane to cyclohexanol and cyclohexanone (KA oil) has attracted much attention because KA oil is irreplaceable in the synthesis of *ε*-caprolactam for industrial production of nylon. Conventional processes employed for cyclohexane oxidation to KA oil are conducted under relatively high temperature and high O₂ pressure. With increasing environmental concerns there is a need to develop green and efficient processes to replace the existing ones. It is considered that photocatalysis that uses solar energy and inexpensive O₂ should provide a green and economical way to produce KA oil. There

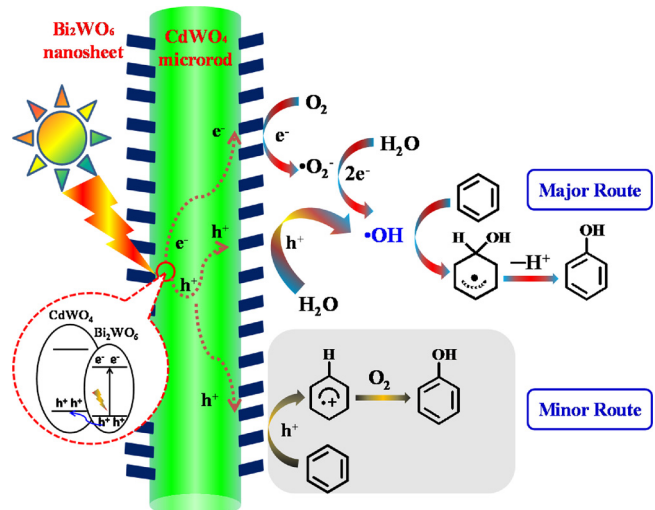


Fig. 4. Plausible mechanism of photocatalytic benzene hydroxylation to phenol over the hierarchical heterostructure of Bi₂WO₆/CdWO₄. [After Appl. Catal. B: Environ. 234 (2018) 311–317].

were significant progresses in the selective oxidation of organics in the last century, especially since the 1970s [62]. Investigation on the use of photocatalysts for the oxidation of cyclohexane, however, only started at the beginning of the 21st century, and the development of a photocatalyst that is highly efficient for the task is still the key of this issue. Among the studied photocatalysts for such a goal, TiO₂ showed high activity but low selectivity to KA oil owing to over oxidation. The formation of carbonates and carboxylates on the surface slows down desorption of cyclohexanone and cyclohexanol and thus leads to their deep oxidation to CO₂ and H₂O [63]. To prevent over oxidation, Almeida et al. modified the surface of commercial TiO₂ with trimethylsilane, Si(CH₃)₃. Below 1.0 wt% Si content, there was decrease of formation rate of KA oil due to the loss of surface OH. It was when Si content was higher than 1.0 wt% that cyclohexanone TOF became higher than that of unmodified TiO₂. It is apparent that there is an optimal presence of Si(CH₃)₃ so that the negative effect of surface OH loss can not only be compensated but also surpassed by the dominance of product desorption [64]. Furthermore, a combination with another metal oxide can result in enhancement of photocatalytic activity as well as product selectivity over TiO₂. The work of Yang et al. revealed that despite V₂O₅ by itself is photocatalytically inactive, the deposition of V₂O₅ on TiO₂ resulted in 18.9% cyclohexane conversion and nearly 100% KA oil selectivity under simulated light irradiation [65]. It was pointed out that the kind of solvents has an effect on both activity and selectivity. In this reaction, it is h⁺ and ·O₂[−] rather than ·OH radicals that are responsible for the formation of KA oil. It is unfortunate that the authors did not explain why there is no detection of over-oxidized product such as CO₂ in the presence of ·OH and ·O₂[−] radicals. In 2012, Ide and coworkers reported the use of Fe-modified TiO₂ (FeO@TiO₂ and FeO_{0.13}-Layered titanate) as photocatalysts under CO₂ atmosphere for the selective oxidation of cyclohexane. The adsorbed CO₂ on the surface of catalyst promoted desorption of cyclohexanol and cyclohexanone and hence lessened deep oxidation of products [66,67]. In 2016, the same research group prepared mesoporous silica that was decorated with isolated tetrahedrally coordinated Ti and Fe oxide nanoparticles on the pore surface for KA oil production under O₂ and solar light irradiation. They confirmed that there was Ti–O–Fe bond formation between Ti species and Fe oxide nanoparticles, which is beneficial for the transfer of electrons from Fe oxide to the adjacent Ti⁴⁺, resulting in the formation of excited species and recombination suppression of photogenerated charge carriers. The as-prepared composite showed cyclohexane conversion of 2.3% and product selectivity of near 100% under solar light irradiation. They attributed the results to the

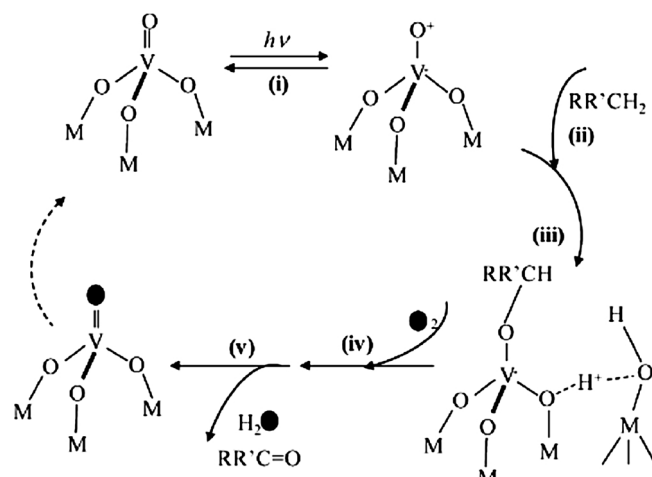


Fig. 5. Photocatalytic cycle for selective oxidation of hydrocarbon to ketone over orthovanadate-like ($V = O$) O_3 species. [After J. Phys. Chem. C 113 (2009) 17018–17024].

lengthened lifetime of active Ti species and visible light induced activity displayed by the Fe oxide nanoparticles [68]. Using Cr/Ti/Si ternary and Cr/Si binary mixed oxides as photocatalysts and on the basis of the obtained results, Shiraishi and coworkers proposed a three-step reaction process: first there is electron transfer from terminal O^{2-} to Cr^{6+} , resulting in excitation of Cr^{6+} species, then the resulting electrophilic O^- attracted a H atom of cyclohexane to produce cyclohexyl radical, finally the excited species react with O_2 to produce the partially oxidized products [69–71].

Besides TiO_2 -based photocatalysts, there are others that were investigated for the generation of KA oil. In 2004, Tanaka and coworkers reported a V_2O_5/Al_2O_3 composite photocatalyst that showed KA oil selectivity up to 87% and K/A ratio of 3.8 in the oxidation of cyclohexane [72]. Irradiation of solar light would result in activity higher than that of visible light irradiation but the UV light of the former caused over oxidation of cyclohexane to CO_2 . The reaction mechanism over this composite is different from that of traditional photocatalysis. It was orthovanadate-like ($C=O$) O_3 species rather than photogenerated holes that activate cyclohexane to produce an alkoxide intermediate which reacts with molecular O_2 to produce KA oil and water [73] (Fig. 5). In the study of photocatalytic oxidation of cyclohexane with O_2 over WO_3 loaded with Pt nanoparticles (Pt/WO_3) under irradiation of visible light, Shiraishi et al. pointed out that the photo-formed electrons on the conduction band of WO_3 were consumed in multi-electron reduction of O_2 on the Pt particles, forming H_2O and H_2O_2 as a result. With the formation of $•O_2^-$ prevented, the generation of KA oil was enhanced [74]. In view of the formation of superoxide anion $•O_2^-$ on TiO_2 -based photocatalysts would result in over oxidation of intermediate and products, Shiraishi et al. hybridized TiO_2 with reduced graphene oxide (rGO) to suppress one-electron reduction of O_2 . As shown in Fig. 6, there is the transfer of photogenerated electrons from the CB of TiO_2 to rGO, and the electrons on rGO promote two-electron rather than one-electron reduction of O_2 [75].

Recently, significant advances were made by Kang and coworkers. In 2014, they reported the use of metal (Ag, Au or Cu) nanoparticles/carbon quantum dots (CQD) composites for KA oil production using H_2O_2 as oxidant, with Au/CQDs being the highest in activity (63.8% cyclohexane conversion) as well product selectivity (99.9%). The selective oxidation of cyclohexane occurred at the interface between Au and CQDs. They attributed the high activity and selectivity to the presence of Au that enhanced light absorption by surface plasma resonance, and the production of $•OH$ from H_2O_2 decomposition [76]. In the same year, they disclosed a photocatalytic system in which H_2O_2 was produced in situ from H_2O using Au/C_3N_4 composite as

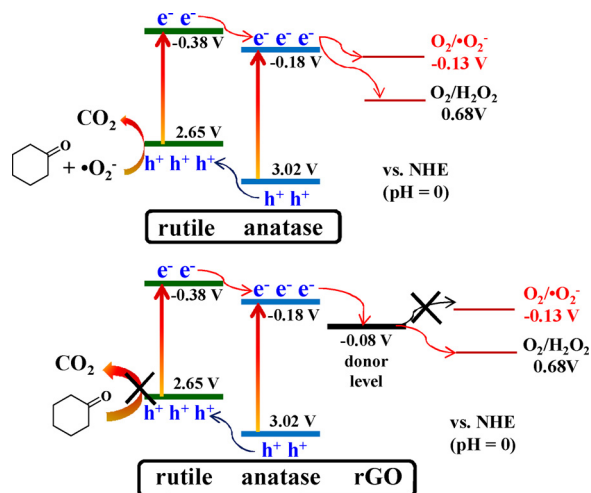


Fig. 6. Energy diagrams for (a) TiO_2 and (b) TiO_2/rGO . [After ACS Catal. 7 (2017) 293–300].

photocatalyst under visible light irradiation in a N_2 atmosphere. The conversion of cyclohexane was 10.54% and selectivity to cyclohexanone 100%. Despite cyclohexane conversion is not as high as that using H_2O_2 as oxidant and Au/CQDs as photocatalyst, the catalytic efficiency is much higher than that of industrial route (conversion limited to 4% with selectivity not higher than 80%). In this system, C_3N_4 acts as an irreplaceable facilitator for H_2O_2 generation. Using water as solvent and without any need of oxidants or initiators, the green process has much potential in industrial applications [77] (Fig. 7). Recently, they fabricated polytriazine imide (PTI, with structure similar to that of C_3N_4) and used it as photocatalyst for cyclohexane oxidation in water and under air atmosphere. Unlike C_3N_4 , PTI could be excited under light irradiation, and the photogenerated holes on the valence band interact with H_2O to produce $•OH$. In this green reaction system, oxygen and water turn into superoxide and hydroxyl radicals on the conduction and valence band of PTI, respectively, leading to 5.81% cyclohexane conversion and 99.9% selectivity to cyclohexanone [78].

Most recently, bismuth-containing semiconductors aroused tremendous attention among scientists because most of them show visible light absorption ability. As reported by Henriquez et al. [79], $BiOX$ ($X = Cl, Br, I$) acted as efficient photocatalysts for partial oxidation of cyclohexane to KA oil. Over $BiOX$, selectivity to cyclohexanol is significantly higher than that over TiO_2 , Fe-doped TiO_2 and N-doped TiO_2 photocatalysts (cyclohexanone/cyclohexanol = 4.49–87.5), especially in the case of $BiOI$ (cyclohexanone/cyclohexanol = 0.23). It is worth pointing out that unlike the other cases, only trace amount of CO_2 was detected when $BiOI$ was used as photocatalyst. The phenomenon could

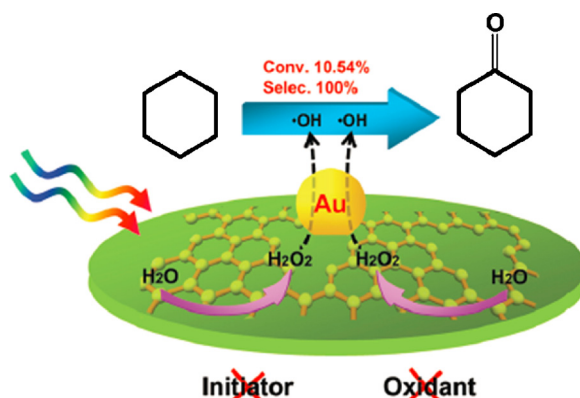


Fig. 7. Proposed reaction mechanism for visible light driven oxidation of cyclohexane over C_3N_4/Au . [After Green Chem. 16 (2014) 4559–4565].

Table 3

Summary of lately developed photocatalysts and their performance in the selective oxidation of cyclohexane.

Entry	Photocatalyst	Reaction conditions	Conv.	KA oil		Ref.
				Sele./%	one/ol	
1	0.01-V ₂ O ₅ @TiO ₂ (100 mg)	500 W Xe Lamp, O ₂ , MeCN + H ₂ O solvent, 4 h	12.4	> 99.9	5.5	[66]
2	FeO _{0.13} -TLO (30 mg)	500 W Xe Lamp, O ₂ , MeCN solvent, 6 h	0.22	> 99.9	0.89	[67]
3	Fe _{0.2} Ti _{0.02} -SBA (60 mg)	500 W Xe Lamp, O ₂ (250 kPa), MeCN solvent, 48 h	2.3	> 99.9	0.59	[69]
4	Cr _{0.04} Ti _{0.04} Si (50 mg)	λ > 400 nm, O ₂ , MeCN solvent, 5 h	–	98.8	3.3	[70]
5	V ₂ O ₅ /Al ₂ O ₃ (100 mg)	500 W Hg lamp, O ₂ , 24 h	0.63	86.0	4.4	[74]
6	TiO ₂ /rGO _{1.0} (20 mg)	2000 W Xe Lamp (λ > 400 nm), O ₂ (1 atm), 12 h	–	83.0	14.8	[75]
7	Pt(0.2)/WO ₃ (10 mg)	λ > 420 nm, O ₂ (1 atm), MeCN solvent, 12 h	–	94	1.1	[76]
8	Au/CQDs (25 mg)	Xe Lamp λ > 420 nm, H ₂ O ₂ (3:1), 48 h	63.8	> 99.9	Almost Cy-one	[78]
9	PTI (150 mg)	300 W Xe Lamp, H ₂ O and air, 48 h	5.81	> 99.9	Almost Cy-one	[80]

be related to the narrow band gap and lower oxidation capacity of BiOI. What is more, TiO₂ and the TiO₂-based catalysts are higher than BiOX in ability for cyclohexanol adsorption, which is another reason for the higher selectivity to cyclohexanone and CO₂ over the latter. In our group, we found Bi₂MoO₆ showed relatively high activity for cyclohexane oxidation but over oxidation was significant owing to the strong oxidation ability of h⁺ on its valance band. We hybridized Bi₂MoO₆ with g-C₃N₄ to regulate the oxidation capacity. With the generation of heterojunctions between the two components, the photo-formed h⁺ transferred from the VB of Bi₂MoO₆ to g-C₃N₄. Under visible light irradiation, there was no detection of CO₂ and the amount of KA oil produced was admirable, and the cyclohexanone/cyclohexanol ratio was close to one.

Overall, there are systems efficient for selective oxidation of cyclohexane to KA oil. As a matter of fact, in laboratory scale some of them show performance better than that of the currently adopted industrial processes (Table 3). However, to the best of our knowledge, none of them have been scaled up for KA oil production. Despite the research achievements, the photocatalytic processes still have a long way to go before industrialization. There are technical problems to overcome such as the design of reactors for efficient light transfer and utilization.

2.4. Selective oxidation of C(sp³)-H in alkanes

The selective activation and oxidation of primary carbon-hydrogen, i.e. C(sp³)-H bonds of alkanes has great potentials in applied chemistry. It is an economical way to produce value-added products from natural petroleum [80]. However, the C(sp³)-H bonds are thermodynamically strong and kinetically inert, and oxygen is a relatively unreactive molecule at mild conditions. The traditional catalytic strategies for the activation of C(sp³)-H bonds require the use of toxic, aggressive and expensive reagents under rather stringent conditions [81]. What is worse is that there is limitation in reactant conversion and product selectivity [82]. From the standpoint of green and sustainable chemistry, it is ideal to use inexhaustible solar energy as driving force and oxygen as oxidant for the activation and oxidation of primary carbon-hydrogen bonds. Recently, the partial oxidation of toluene has received much attention because the products are needed for the synthesis of commodities such as pharmaceuticals, photosensitizers, flavors, and fragrances. The typical results are summarized and listed in Table 4. It is apparent that TiO₂ shows the lowest selectivity to aldehydes no matter it is modified or not.

It was reported that under UV irradiation, TiO₂ functions as a photocatalyst for selective oxidation of toluene. As reported by Ouidri et al. [83] and Cao et al. [84], the activity of TiO₂ is closely related to

specific surface area, exposed facets as well as reaction conditions (e.g. nature of solvents). The yield of benzaldehyde was up to 48% over TiO₂-pillared montmorillonite, and by-products such as benzyl alcohol, benzoic acid, pyrogallol and hydroquinone were detected [83]. The presence of by-products is unwelcome in industry because it is costly to have them separated. To enhance selectivity to benzaldehyde, Tripathy and coworkers [85] modified TiO₂ with Pt, Pd and Ru, and among the three the Ru-loaded one showed the highest benzaldehyde selectivity. In the presence of O₂, the generation of •O₂[−] always results in oxidation of target products. As shown in Fig. 8, the Ru^{3+/4+} states in TiO₂ are situated at 0.4 eV below the conduction band of anatase, and the electrons trapped on these states are not energetic enough to create •O₂[−] from O₂. Instead, there is transfer of electrons form the CB of TiO₂ to that of Ru^{3+/4+} states and the pathway for •O₂[−] generation is terminated. Consequently, oxidation step 3 is prevented and there is no further oxidation of the target products (Fig. 8). In another case of promoting benzaldehyde selectivity, Shiraiishi and coworkers loaded TiO₂ with WO₃, and benzaldehyde selectivity was improved from 12% to 50% [86]. On WO₃/TiO₂, the active sites responsible for oxidation are located on the exposed TiO₂ surface. Once these active sites are partially blocked by WO₃ that is much less active, the photocatalytic decomposition of benzaldehyde on TiO₂ is suppressed, resulting in high benzaldehyde selectivity.

One of the drawbacks of the above photocatalytic approaches is the use of UV light. In 2013, Yuan and coworkers reported the use of chlorinated BiOBr-TiO₂ for the selective activation of primary carbon-hydrogen under visible light irradiation [87]. In this system, BiOBr acts as sensor for visible light absorption to produce electrons and holes on the valance band (VB) of TiO₂. Induced by the VB holes, there is the generation of •Cl radicals from chlorine. As main active species in BTF solution, •Cl radicals react with alkanes to generate alkyl radicals. It was pointed out that owing to the ample presence of O₂ on the surface of photocatalyst as well as in the solution, the formation of alkyl halides from •Cl and alkyl radicals is prohibited (Fig. 9). Compared to BiOBr/TiO₂, the chlorination of BiOBr/TiO₂ resulted in an increase of toluene conversion from 0.12% to 1.8%. This work of Yuan and coworkers provides a photocatalytic strategy for direct C(sp³)-H functionalization under mild conditions. Nonetheless, the method is not practical because the activity is low and the presence of Cl[−] would raise operational cost.

As one of the most commonly used visible light driven photocatalysts, CdS 2D nanomaterials also showed high activity for the partial oxidation of toluene into benzaldehyde under visible light irradiation [88]. Owing to the proper band gap structure, the selectivity (no detection of other by-products) to benzaldehyde was extremely high. However, the reaction was conducted in the presence of benzotrifluoride solvent which will add cost for separation. In our group, we

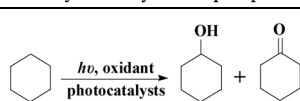


Table 4

Summary of lately developed photocatalysts and their performance on the selective oxidation of toluene into benzaldehyde.

Entry	Photocatalyst	Reaction conditions	Sel./%	Formation rate ($\mu\text{mol/g/h}$)	Ref.
1	TiO ₂ -pillared clays (50 mg)	Hg lamp $\lambda > 340$ nm, H ₂ O, 1h	65.3	1040	[83]
2	1 at% Ru-TiO ₂ (0.78 cm ²)	He-Cd Laser $\lambda = 325$ nm, O ₂ , 4h	89.1	–	[85]
3	Cl-BiOBr/TiO ₂ (20 mg)	$\lambda > 420$ nm, O ₂ (0.1 MPa), benzotrifluoride solvent, 12h	94	662	[87]
4	Bi ₂ WO ₆ (50 mg)	$\lambda > 400$ nm, O ₂ (3 mL/min), 5h	96	464	[93]
5	0.1 wt% Pd/Bi ₂ WO ₆ (50 mg)	$\lambda > 400$ nm, O ₂ (1 atm), 5h	90	1140	[94]
6	CdS (10 mg)	40 W watt CFL lamp, benzotrifluoride solvent, 1.5 h	100	667	[88]
7	Cd ₃ (TMT) ₂ /CdS (50 mg)	$\lambda > 420$ nm, O ₂ (1.5 mL/min), 3h	98.5	787	[89]
8	W ₁₈ O ₄₉ (50 mg)	$\lambda > 420$ nm, O ₂ (1 atm), benzene solvent, 22 h	–	477	[28]
9	VO@g-C ₃ N ₄ (10%V, 25 mg)	40 W domestic bulb, H ₂ O ₂ , MeCN solvent, 12 h	–	4700	[92]
10	Bi self-doped Bi ₂ MoO ₆ -Bi ₂ Mo ₃ O ₁₂ (100 mg)	$\lambda > 400$ nm, O ₂ (3 mL/min), benzotrifluoride (3 mL), 3h	98.5	508	[95]

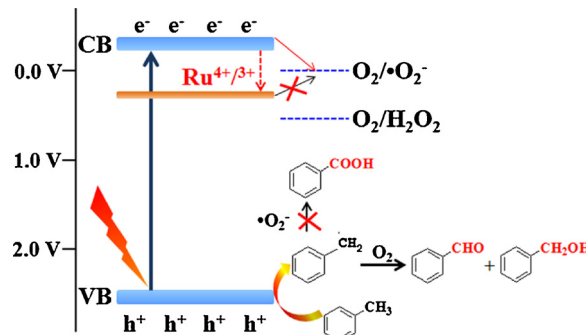


Fig. 8. Illustration of band position on TiO₂ and Ru-doped TiO₂ during toluene oxidation and proposed reaction pathway. [After Angew. Chem. Int. Ed. 53 (2014) 12605–12608].

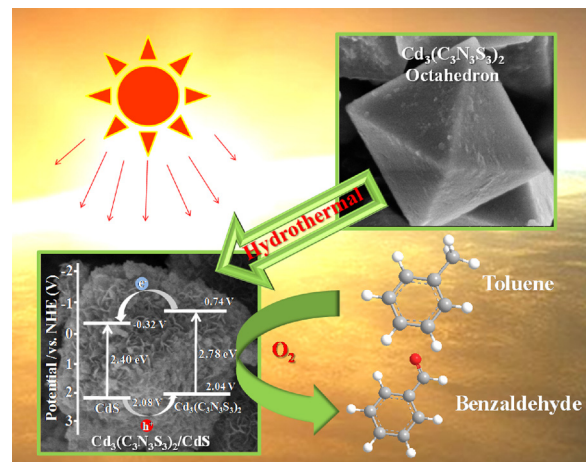


Fig. 10. Toluene oxidation over porous Cd₃(C₃N₃S₃)₂/CdS composite without the addition of any solvent under visible light irradiation. [After Appl. Catal. B: Environ. 233 (2018) 243–249].

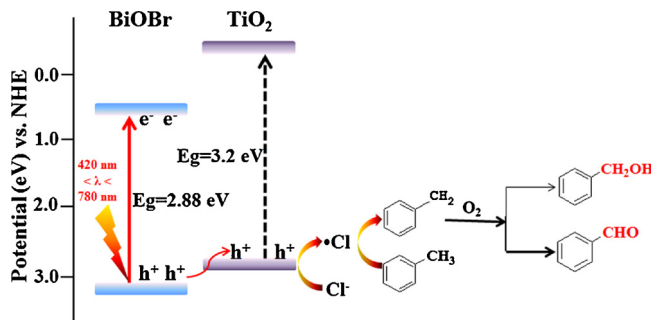


Fig. 9. Proposed mechanism for the chlorine-radical-mediated photocatalytic activation of hydrocarbons and further functionalization. [After Angew. Chem. Int. Ed. 52 (2013) 1035–1039].

developed a facile hydrothermal method to prepare novel porous Cd₃(C₃N₃S₃)₂/CdS composite that showed high activity and selectivity for the selective oxidation of toluene into benzaldehyde without the need of any solvent (Fig. 10) [89]. The Cd₃(C₃N₃S₃)₂/CdS composite was synthesized by a simple hydrothermal approach using Cd₃(C₃N₃S₃)₂ as precursor. It is envisaged that the method is suitable for the generation of other organic/inorganic composites for photocatalytic purposes.

With proper band gap energy, g-C₃N₄ is widely used in organic synthesis, especially in the selective oxidation of alkyl alcohols. Most recently, g-C₃N₄ was tested for the activation of sp³ C-H bonds, and in spite of the high selectivity to partial oxidation products, activity was poor when O₂ was used as oxidant. Nonetheless, through methods such

as doping with carbon nanodots [90], and modification with N-hydroxy [91] or VO [92], there was improvement in activity. For example, using H₂O₂ as oxidant and MeCN as solvent, the oxidation of methyl arenes and their analogues over a VO@g-C₃N₄ composite resulted in excellent yields of the corresponding carbonyl compounds and phenols after 8 h under visible light irradiation [92].

Considering the strong visible light absorption ability of bismuth-containing semiconductors, our group prepared a series of bismuth-based materials and investigated their photocatalytic activity in selective oxidation of alkanes. We first prepared flower-like Bi₂WO₆ that showed high selectivity (up to 100%) in the partial oxidation of toluene and its derivatives [93]. The generation of benzyl radicals through h⁺ interaction with reactants was critical. Despite high selectivity to aldehydes, reaction activity was low and catalyst reusability poor. Furthermore, the loss of flower-like morphology would result in loss of activity. To find ways to improve catalyst stability, it is critical to gain insight into the cause of morphology collapse and how such a collapse would affect catalytic activity. Similar results were reported by Li's group [94]. However, with the loading of Pd on the surface of flower-like Bi₂WO₆, there was improved activity owing to the efficiency in the separation of charge carriers.

Recently, we prepared a stable Bi self-doping Bi₂MoO₆-Bi₂Mo₃O₁₂ composite by a simple hydrothermal method and used it as photocatalyst for the activation of C(sp³)-H bonds [95]. With doping of Bi

into the composite, the valance band of bismuth molybdates becomes more negative in position, which is an indication of lower oxidation capacity. With proper Bi doping, the production of benzaldehyde reaches 508 µmol/g/h with selectivity higher than 98.5%. It is worth pointing out that the composite showed high stability even after six reaction cycles. To further improve toluene conversion, we modified porous C₃N₄ with spatially separated Ag and Co₃O₄ adopting a supramolecular assembly method. Using toluene as raw material and together with the reaction between benzaldehyde and halobenzene, the conversion of toluene reached 80% and the selectivity to ketones up to 99%. This study provides a new route for the preparation of important intermediates such as of bifonazoles under mild conditions.

3. Summary and perspective

Photocatalytic reactions can be conducted under mild reaction conditions using inexhaustible solar energy. The oxidation capacity of photocatalysts can be regulated through band-gap engineering of semiconductors, and extremely high selectivity to target product could be achieved. Nonetheless, despite much effort the lack of efficient photocatalysts is still the bottleneck for industrialization of photocatalytic technology. According to the above discussions, factors that have an effect on the activity of a heterogeneous photocatalyst can be divided into two categories: physicochemical properties and reaction conditions. Physicochemical properties such as phase structure, band gap position, light absorption ability, surface/interface structure, defect, and morphology, vary greatly with preparation methods, and even a little change in preparation procedure may result in grand difference in photocatalytic activity. The performance of a photocatalyst in terms of activity and selectivity is also governed by reaction conditions such as light intensity and source, solvent, oxidant and reactor. Because of the complexity of multi-effects and photocatalytic procedures, it is hard to establish a relationship between catalytic performance and a particular factor. In addition, with the unsatisfactory photocatalytic activity for organic synthesis, there is almost no attempt on scaled-up processes as well as design of reactors.

There are several areas that should be targeted on in the future: (1) For rational design of photocatalysts and improvement of photocatalytic activity, it is essential to understand reaction mechanism, especially that related to the participation of active species. As depicted in the discussion conducted so far, ·O₂⁻ has been regarded as efficient species for high selectivity as well as arch-criminal for low selectivity to target products in selective oxidation of alkanes. The search of active species milder in oxidation capacity such as singlet oxygen could be rewarding. (2) To design photocatalysts of discrete band gap structures is essential for the establishment of relation between oxidation ability and redox potential of semiconductors. For this kind of studies, reactions have to be conducted under some adopted standard reaction conditions. (3) The adsorption of reactant(s) and desorption of product(s) is closely dependent on surface structure of semiconductors. Modifying the surface structure of a photocatalyst is a viable strategy to enhance performance. Through careful study of adsorption-desorption behaviors of reactant(s), intermediate(s) and product(s), the modification can be conducted in a rational manner. This is often neglected because most attentions are paid to the separation of charge carriers. (4) The development of simple and environment-benign methods for scale-up preparation of photocatalysts is critical for industrialization. (5) To cater for future challenges, new materials have to be explored for the development of suitable photocatalysts. (6) The applications of photocatalysis in organic synthesis should be expanded, especially for the synthesis of heat-sensitive organics. (7) To realize industrialization, it is necessary to design suitable reactors for the processes. A thorough understanding of heat, mass and light transfer of a reaction system especially in scale-up reactions is inevitable.

Acknowledgements

This project was financially supported by the NSFC (Grants 21725602, 21776064, 21671062, and 21476065), the Natural Science Foundation of Hunan Province (Grant 2015JJ3033), the Science and Technology Project of Hunan Province (2015JC3051), and the Fundamental Research Funds for the Central Universities (Hunan University). CT Au thanks the HNU for an adjunct professorship.

References

- [1] M. Fujihira, Y. Satoh, T. Osa, *Nature* 293 (1981) 206–208.
- [2] D.A. Nicewicz, D.W.C. MacMillan, *Science* 322 (2008) 77–80.
- [3] B. Konig, *Eur. J. Org. Chem.* 15 (2017) 1979–1981 and references therein.
- [4] M. Zhang, C. Chen, W. Ma, J. Zhao, *Angew. Chem. Int. Ed.* 47 (2008) 9730–9733.
- [5] M. Zhang, Q. Wang, C. Chen, L. Zang, W. Ma, J. Zhao, *Angew. Chem. Int. Ed.* 48 (2009) 6081–6084.
- [6] Q. Wang, M. Zhang, C. Chen, W. Ma, J. Zhao, *Angew. Chem. Int. Ed.* 49 (2010) 7976–7979.
- [7] G. Palmisano, S. Yurdakal, V. Augugliaro, V. Loddo, L. Palmisano, *Adv. Syn. Catal.* 349 (2007) 964–970.
- [8] J.C. Colmenares, W. Ouyang, M. Ojeda, E. Kuna, O. Chernyayeva, D. Lisovitskiy, S. De, R. Luque, A.M. Balu, *Appl. Catal. B: Environ.* 183 (2016) 107–112.
- [9] J.C. Colmenares, A. Magdziarz, O. Chernyayeva, D. Lisovitskiy, K. Kurzydlowski, J. Grozonka, *ChemCatChem* 5 (2013) 2270–2277.
- [10] J.C. Colmenares, A. Magdziarz, K. Kurzydlowski, J. Grozonka, O. Chernyayeva, D. Lisovitskiy, *Appl. Catal. B: Environ.* 134–135 (2013) 136–144.
- [11] Y. Shiraiishi, T. Hirai, J. Photochem. Photobiol. C: Photochem. Rev. 9 (2008) 157–170.
- [12] X. Lang, J. Zhao, X. Chen, *Angew. Chem. Int. Ed.* 55 (2016) 4697–4700.
- [13] X. Li, J.L. Shi, H. Hao, X. Lang, *Appl. Catal. B: Environ.* 232 (2018) 260–267.
- [14] J.L. Shi, H. Hao, X. Li, X. Lang, *Catal. Sci. Technol.* 8 (2018) 3910–3917.
- [15] J.T. Li, S.K. Cushing, P. Zhang, T. Senty, F.K. Meng, A.D. Bristow, A. Manivannan, N.Q. Wu, J. Am. Chem. Soc. 136 (2014) 8438–8449.
- [16] P. Zhang, P. Wu, S. Bao, Z. Wang, B. Tian, J. Zhang, *Chem. Eng. J.* 306 (2016) 1151–1161.
- [17] X. Li, J. Wang, Y. Men, Z. Bian, *Appl. Catal. B: Environ.* 187 (2016) 115–121.
- [18] H. Li, R. Liu, S. Lian, Y. Liu, H. Huang, Z. Kang, *Nanoscale* 5 (2013) 3289–3297.
- [19] S. Verma, R.B.N. Baig, M.N. Nadagouda, R.S. Varma, *ACS Sustainable Chem. Eng.* 4 (2016) 1094–1098.
- [20] F. Su, S.C. Mathew, G. Lipner, X. Fu, M. Antonietti, S. Blechert, X. Wang, *J. Am. Chem. Soc.* 132 (2010) 16299–16301.
- [21] L. Su, X. Ye, S. Meng, X. Fu, S. Chen, *Appl. Surf. Sci.* 384 (2016) 161–174.
- [22] S. Meng, X. Ye, X. Ning, M. Xie, X. Fu, S. Chen, *Appl. Catal. B: Environ.* 182 (2016) 356–368.
- [23] D. Guo, Y. Wang, P. Zhao, M. Bai, H. Xin, Z. Guo, J. Li, *Catal.* 6 (2016) 64.
- [24] C.A. Unsworth, B. Coulson, V. Chechik, R.E. Douthwaite, *J. Catal.* 354 (2017) 152–159.
- [25] H. Li, F. Qin, Z. Yang, X. Cui, J. Wang, L. Zhang, *J. Am. Chem. Soc.* 139 (2017) 3513–3521.
- [26] B. Long, Z. Ding, X. Wang, *ChemSusChem* 6 (2013) 2074–2078.
- [27] K. Tamai, S. Hosokawa, K. Teramura, T. Shishido, T. Tanaka, *Appl. Catal. B: Environ.* 182 (2016) 469–475.
- [28] H. Bai, W. Yi, J. Liu, Q. Lv, Q. Zhang, Q. Ma, H. Yang, G. Xi, *Nanoscale* 8 (2016) 13545–13551.
- [29] M.B. Chambers, X. Wang, L. Ellezam, O. Ersen, M. Fontecave, C. Sanchez, L. Rozes, C. Mellot-Draznieks, *J. Am. Chem. Soc.* 139 (2017) 8222–8228.
- [30] L. Hou, *Nano* 12 (2017) 100–108.
- [31] M. Xie, X. Dai, S. Meng, X. Fu, S. Chen, *Chem. Eng. J.* 245 (2014) 107–116.
- [32] Q. Yuan, Z. Wu, Y. Jin, L. Xu, F. Xiong, Y. Ma, W. Huang, *J. Am. Chem. Soc.* 135 (2013) 5212–5219.
- [33] X. Liang, X. Yang, G. Gao, C. Li, Y. Li, W. Zhang, X. Chen, Y. Zhang, B. Zhang, Y. Lei, Q. Shi, *J. Catal.* 339 (2016) 68–76.
- [34] Q. Xiao, Z. Liu, A. Bo, S. Zavarh, S. Sarina, S. Bottle, J.D. Riches, H. Zhu, *J. Am. Chem. Soc.* 137 (2015) 1956–1966.
- [35] T. Tana, X.W. Guo, Q. Xiao, Y. Huang, S. Sarina, P. Christopher, J. Jia, H. Wu, H. Zhu, *Chem. Commun.* 52 (2016) 11567–11570.
- [36] S. Zavarh, Q. Xiao, S. Sarina, J. Zhao, S. Bottle, M. Wellard, J. Jia, L. Jiang, Y. Huang, J.P. Blinco, H. Wu, H.Y. Zhu, *ACS Catal.* 6 (2016) 3580–3588.
- [37] F. Xie, Y. Zhang, X. He, H. Li, X. Qiu, W. Zhou, S. Huo, Z. Tang, *J. Mater. Chem. A* 6 (2018) 13236–13243.
- [38] D. Bianchi, R. Bortolo, R. Tassinari, M. Ricci, R. Vignola, *Angew. Chem. Int. Ed.* 39 (2000) 4321–4323.
- [39] S. Ito, A. Mitarai, K. Hikino, M. Hirama, K. Sasaki, *J. Org. Chem.* 57 (1992) 6937–6941.
- [40] X. Chen, J. Zhang, X. Fu, M. Antonietti, X. Wang, *J. Am. Chem. Soc.* 131 (2009) 11658–11659.
- [41] T. Matsuura, K. Omura, *Synthesis* 3 (1974) 173–184 and references therein.
- [42] Y. Ide, N. Nakamura, H. Hattori, R. Ogino, M. Ogawa, M. Sadakane, T. Sano, *Chem. Commun.* 47 (2011) 11531–11533.
- [43] Z. Zheng, B. Huang, X. Qin, X. Zhang, Y. Dai, M.H. Whangbo, *J. Mater. Chem.* 21 (2011) 9079–9087.

- [44] H. Yuzawa, M. Aoki, K. Otake, T. Hattori, H. Itoh, H. Yoshida, *J. Phys. Chem. C* 116 (2012) 25376–25387.
- [45] P. Devaraji, N.K. Sathu, C.S. Gopinath, *ACS Catal.* 4 (2014) 2844–2853.
- [46] E. Taylor, O. Buchardt, *Chem. Rev.* 70 (1970) 231–265.
- [47] X. Ye, Y. Cui, X. Qiu, X. Wang, *Appl. Catal. B: Environ.* 152–153 (2014) 383–389.
- [48] P. Zhang, Y. Gong, H. Li, Z. Chen, Y. Wang, *RSC Adv.* 3 (2013) 5121–5126.
- [49] B. Xu, Z. Chen, B. Han, C. Li, *Catal. Commun.* 98 (2017) 112–115.
- [50] D. Wang, M. Wang, Z. Li, *ACS Catal.* 5 (2015) 6852–6857.
- [51] K.I. Shimizu, T. Komokazu, T. Fujishima, T. Kodama, H. Yoshida, Y. Kitayama, *Appl. Catal. A: Gen.* 225 (2002) 185–191.
- [52] R. Su, L. Kesavan, M.M. Jensen, R. Tiruvalam, Q. He, N. Dimitratos, S. Wendt, M. Glasius, C.J. Kiely, G.J. Hutchings, F. Besenbacher, *Chem. Commun.* 50 (2014) 12612–12614.
- [53] H. Yuzawa, H. Yoshida, *Top. Catal.* 57 (2014) 984–994.
- [54] T.D. Bui, A. Kimura, S. Ikeda, M. Matsumura, *J. Am. Chem. Soc.* 132 (2010) 8453–8458.
- [55] Y. Shiraishi, N. Saito, T. Hirai, *J. Am. Chem. Soc.* 127 (2005) 12820–12822.
- [56] G. Zhang, J. Yi, J. Shim, J. Lee, W. Choi, *Appl. Catal. B: Environ.* 102 (2011) 132–139.
- [57] R. Asahi, T. Morikawa, T. Ohwaki, K. Aoki, Y. Taga, *Science* 293 (2001) 269–271.
- [58] T. Morikawa, Y. Irokawa, T. Ohwaki, *Appl. Catal. A: Gen.* 314 (2008) 123–127.
- [59] H. Irie, K. Kamiya, T. Shibanuma, S. Miura, D.A. Tryk, T. Yokoyama, K. Hashimoto, *J. Phys. Chem. C* 113 (2009) 10761–10766.
- [60] O. Tomita, B. Ohtni, R. Abe, *Catal. Sci. Technol.* 4 (2014) 3850–3860.
- [61] P. Chen, L. Chen, Y. Zeng, F. Ding, X. Jiang, N. Liu, C.T. Au, S.F. Yin, *Appl. Catal. B: Environ.* 234 (2018) 311–317.
- [62] P. Pichat, *Catal. Today* 19 (1994) 313–333.
- [63] A.R. Almeida, J.A. Moulijn, G. Mul, *J. Phys. Chem. C* 112 (2008) 1552–1561.
- [64] A.R. Almeida, J.T. Carneiro, J.A. Moulijn, G. Mul, *J. Catal.* 273 (2010) 116–124.
- [65] D. Yang, T. Wu, C. Chen, W. Guo, H. Liu, B. Han, *Green Chem.* 19 (2017) 311–318.
- [66] H. Hattori, Y. Ide, S. Ogo, K. Inumaru, M. Sadakane, T. Sano, *ACS Catal.* 2 (2012) 1910–1915.
- [67] Y. Ide, H. Hattori, S. Ogo, M. Sadkane, T. Sano, *Green Chem.* 14 (2012) 1264–1267.
- [68] Y. Ide, M. Iwata, Y. Yagenji, N. Tsunooji, M. Sohmiya, K. Komaguchi, T. Sano, Y. Sugahara, *J. Mater. Chem. A* 4 (2016) 15829–15835.
- [69] D. Tsukamoto, A. Shiro, Y. Shiraishi, T. Hirai, *J. Phys. Chem. C* 115 (2011) 19782–19788.
- [70] Y. Shiraishi, H. Ohara, T. Hirai, *New J. Chem.* 34 (2010) 2841–2846.
- [71] Y. Shiraishi, Y. Teshima, T. Hirai, *Chem. Commun.* 36 (2005) 4569–4571.
- [72] K. Teramura, T. Tanaka, M. Kani, T. Hosokawa, T. Funabiki, *J. Molecular Catal. A: Chem.* 208 (2004) 299–305.
- [73] K. Teramura, T. Ohuchi, T. Shishido, T. Tanaka, *J. Phys. Chem. C* 113 (2009) 17018–17024.
- [74] Y. Shiraishi, Y. Sugano, S. Ichikawa, T. Hirai, *Catal. Sci. Technol.* 2 (2012) 400–405.
- [75] Y. Shiraishi, S. Shiota, H. Hirakawa, S. Tanaka, S. Ichikawa, T. Hirai, *ACS Catal.* 7 (2017) 293–300.
- [76] R. Liu, H. Huang, H. Li, Y. Liu, J. Zhong, Y. Li, S. Zhang, A. Kang, *ACS Catal.* 4 (2014) 328–336.
- [77] J. Liu, Y. Yang, N. Liu, Y. Liu, H. Huang, Z. Kang, *Green Chem.* 16 (2014) 4559–4565.
- [78] Y. Zhang, L. Hu, C. Zhu, J. Liu, H. Huang, Y. Liu, Z. Kang, *Catal. Sci. Technol.* 6 (2016) 7252–7258.
- [79] A. Henriquez, H.D. Mansilla, A.M.M. Cruz, J. Freer, D. Contreras, *Appl. Catal. B: Environ.* 206 (2017) 252–262.
- [80] F. Recuperio, C. Punta, *Chem. Rev.* 107 (2007) 3800–3842.
- [81] L. Kesavan, R. Tiruvalam, M.H.A. Rahim, M.I. Saiman, D.I. Enache, R.L. Jenkins, N. Dimitratos, J.A. Lopez-Sanchez, S.H. Taylor, D.W. Knight, C.J. Kiely, G.J. Hutchings, *Science* 331 (2011) 195–199.
- [82] D. Balcells, E. Clot, O. Eisenstein, *Chem. Rev.* 110 (2010) 749–823.
- [83] S. Ouidri, H. Khalaf, *Photochem. Photobiol. A: Chem.* 207 (2009) 268–273.
- [84] F.L. Cao, J.G. Wang, F.J. Lv, D.Q. Zhang, Y.N. Huo, G.S. Li, H.X. Li, J. Zhu, *Catal. Commun.* 12 (2011) 946–950.
- [85] J. Tripathy, K. Lee, P. Schmuki, *Angew. Chem. Int. Ed.* 53 (2014) 12605–12608.
- [86] D. Tsukamoto, Y. Shiraishi, T. Hirai, *Catal. Sci. Technol.* 3 (2013) 2270–2277.
- [87] R. Yuan, S. Fan, H. Zhou, Z. Ding, S. Lin, Z. Li, Z. Zhang, C. Xu, L. Wu, X. Wang, X. Fu, *Angew. Chem. Int. Ed.* 52 (2013) 1035–1039.
- [88] S.K. Pahari, P. Pal, D.N. Srivastava, S.C. Ghosh, A.B. Panda, *Chem. Commun.* 51 (2015) 10322–10325.
- [89] J. He, L. Chen, D. Ding, Y.K. Yang, C.T. Au, S.F. Yin, *Appl. Catal. B: Environ.* 233 (2018) 243–249.
- [90] W.Y. Zhang, A. Barriotaki, I. Smonou, F. Hollmann, *Green Chem.* 19 (2017) 2096–2100.
- [91] P. Zhang, Y. Wang, J. Yao, C. Wang, C. Yan, M. Antonietti, H. Li, *Adv. Synth. Catal.* 353 (2011) 1447–1451.
- [92] S. Verma, R.B. Nasir Baig, M.N. Nadagouda, R.S. Varma, *ACS Sustain. Chem. Eng.* 4 (2016) 2333–2336.
- [93] Y. Liu, L. Chen, Q. Yuan, J. He, C.T. Au, S.F. Yin, *Chem. Commun.* 52 (2016) 1274–1277.
- [94] B. Yuan, B. Zhang, Z. Wang, S. Lu, J. Li, Y. Liu, C. Li, *Chin. J. Catal.* 38 (2017) 440–446.
- [95] L.N. Song, L. Chen, J. He, P. Chen, H.K. Zeng, C.T. Au, S.F. Yin, *Chem. Commun.* 53 (2017) 6480–6483.